Climate Dynamics (2006) 26: 273–284
DOI 10.1007/s00382-005-0063-y

**Amaelle Landais · Valérie Masson-Delmotte
Jean Jouzel · Dominique Raynaud · Sigfus Johnsen
Christof Huber · Markus Leuenberger
Jakob Schwander · Bénédicte Minster**

The glacial inception as recorded in the NorthGRIP Greenland ice core: timing, structure and associated abrupt temperature changes

Received: 29 September 2004 / Accepted: 27 July 2005 / Published online: 3 September 2005

Abstract The mechanisms involved in the glacial inception are still poorly constrained due to a lack of high resolution and cross-dated climate records at various locations. Using air isotopic measurements in the recently drilled NorthGRIP ice core, we show that no evidence exists for stratigraphic disturbance of the climate record of the last glacial inception (~123–100 kyears BP) encompassing Dansgaard–Oeschger events (DO) 25, 24 and 23, even if we lack sufficient resolution to completely rule out disturbance over DO 25. We quantify the rapid surface temperature variability over DO 23 and 24 with associated warmings of 10 ± 2.5 and 16 ± 2.5°C, amplitudes which mimic those observed in full glacial conditions. We use records of $\delta^{18}O$ of O_2 to propose a common timescale for the NorthGRIP and the Antarctic Vostok ice cores, with a maximum uncertainty of 2,500 years, and to examine the interhemispheric sequence of events over this period. After a synchronous North–South temperature decrease, the onset of rapid events is triggered in the North through DO 25. As for later events, DO 24 and 23 have a clear Antarctic counterpart which does not seem to be the case for the very first abrupt warming (DO 25). This information, when added to intermediate levels of CO_2 and to the absence of clear ice rafting associated with DO 25, highlights the uniqueness of this first event, while DO 24 and 23 appear similar to typical full glacial DO events.

A. Landais (✉) · V. Masson-Delmotte · J. Jouzel · B. Minster
IPSL/Laboratoire des Sciences du Climat et de l'Environnement, UMR CEA-CNRS, CEA Saclay, 91191 Gif-sur -Yvette, France
E-mail: landais@vms.huji.ac.il
Tel.: +33-972-26584246
Fax: +33-972-25662581

D. Raynaud
LGGE, UMR CNRS-UJF, 2 –53 Rue Molière, 38 402 St Martin d'Heres, France

S. Johnsen
Department of Geophysics, University of Copenhagen, Juliane Maries Vej 30, 2100 Copenhagen, Denmark

C. Huber · M. Leuenberger · J. Schwander
Physics Institute, University of Bern, Sidlerstrasse 5, 3012 Bern, Switzerland

A. Landais
Institute of Earth Sciences, Hebrew University, Givat Ram, 91904 Jerusalem, Israel

1 Introduction

Marine and continental records from the Northern Hemisphere have shown that the last glacial period was characterized by rapid climatic variability (e.g. Bond et al. 1993; Genty et al. 2003). The GRIP and GISP2 ice cores (Dansgaard et al. 1984, 1993; Grootes et al. 1993) depict a continuous and high-resolution record of such climatic variability associated with large temperature changes over Greenland (up to 16°C within ~100 years; Lang et al. 1999). When a common age scale can be established, Blunier et al. (1998, 2001) suggest that the Greenlandic rapid events are visible in Antarctica with a different shape: the temperature begins to increase slowly in the South before the abrupt Greenland warming (seesaw mechanism) (Broecker 1998; Stocker and Johnsen 2003).

The recently drilled NorthGRIP Greenland ice core provides the first continuous climatic record of the glacial inception over Greenland (NorthGRIP community members 2004). Unlike the previous ice core records (GRIP and GISP2) that were affected by ice mixing near the bedrock, i.e. before 100 kyears BP (Chappellaz et al. 1997; Grootes et al. 1993), this new $\delta^{18}O_{ice}$ record seems to be undisturbed back to 123 kyears BP. For the first time, the signature of the Dansgaard–Oeschger events (hereafter DO) 23, 24 and 25 can be identified in a

Greenland ice core. If we assume that $\delta^{18}O_{ice}$ is a reliable tool with which to reconstruct past temperature variations (Dansgaard 1964), DO 25 to 21, at the beginning of the glacial period, are associated with smaller temperature increases than the following ones (an average of ~3.5‰ for rapid $\delta^{18}O_{ice}$ increases over DO 24 to 21 instead of ~5‰ for the typical glacial DO 20 to 8). DO 25 shows the weakest $\delta^{18}O_{ice}$ increase, ~1.5‰, i.e. one-third of a typical glacial DO.

Few high-resolution paleoclimatic records including glacial inception are available in the northern Atlantic. The available data indicate that, after a relatively stable interglacial period (Cortijo et al. 1994, 1999), the north Atlantic region was subjected to rapid cooling events. The cold episodes were associated with ice rafting as suggested, in marine cores located north of 40°N, by significant increases of ice-rafted debris (IRD) with a composition typical of the glacial period (Chapman and Shackleton 1999). Such discharge events were called C24 and C23 (Mc Manus et al. 1994; Chapman and Shackleton 1999). In the NorthGRIP ice core, the event C24 (Mc Manus et al. 1994) could be associated with a significant cooling before the warm phase of DO 24 (GS 25, for Greenland Stadial 25; NorthGRIP community paper 2004). In continental and marine records, this event C24 is traditionally associated with the transition between the last interglacial period (stage 5e) and stage 5d (Kukla et al. 2002 and references therein). Going further back in time, the marine core NEAP18K (southeast of Greenland) enabled Chapman and Shackleton (1999) to pinpoint a first IRD signal during the last glacial period, which is four times smaller than the one associated with C24. The authors called it C25 (Fig. 1). In parallel, Mc Manus et al. (2002) and Shackleton et al. (2002) showed that a slight surface cooling without a clear IRD signal is recorded in other North Atlantic cores (Fig. 1). Mc Manus et al. (2002) suggested that it was the same C25 event. However, a $\delta^{18}O_{benthic}$ cross-dating of the different marine cores challenges the synchronicity of the IRD signal and of the surface cooling (Shackleton et al. 2002; Fig. 1). The concordance of the cold phase of DO 25 with an IRD event is therefore still uncertain from marine records.

While no clear record of DO 25 other than the NorthGRIP ice core is available in North Atlantic, the succeeding DO 23 and 24 depicted by IRD and polar fauna signals are similar to the full glacial DO in the northern Atlantic. On the contrary, continental records (e.g. European pollens; Reille et al. 1998; Sanchez-Goñi et al. 1999) show that the period from ~75 to ~115 kyears BP (stages 5a–5d) is associated with a vegetative cover which is intermediate between interglacial and glacial periods (persistence of trees over Europe). Because of the lack of information on DO 25 and of contrasted reconstructions of DO 23 and 24 over land and oceans, Greenland ice cores are the key to a better description of the glacial inception.

The NorthGRIP $\delta^{18}O_{ice}$ provides a much more detailed and better dated climatic record of the glacial inception than continental and marine records. However, $\delta^{18}O_{ice}$ variability remains difficult to quantify in terms of surface temperature changes. First, $\delta^{18}O_{ice}$ rapid variability can be due to stratigraphic disturbances in the ice near the bedrock, as was the case for the GRIP and GISP2 ice cores (Chappellaz et al. 1997; Grootes et al. 1993; Landais et al. 2004a). In the NorthGRIP community members' paper (2004), the main $\delta^{18}O_{ice}$ increase of DO 24 was shown from gas analyses to be of climatic origin but such analyses were not available deeper in the core. Such an investigation is of primary importance since this sequence of the glacial inception is unique among Greenland ice cores. Second, even if the ice stratigraphy is not disturbed, the Greenland $\delta^{18}O_{ice}$ cannot be directly related to surface temperature. Indeed, past changes in (1) precipitation seasonality (Fawcett et al. 1997; Krinner et al. 1997), (2) source temperature (Boyle 1997; Cuffey and Vimeux 2001; Masson-Delmotte et al. 2005a) and (3) surface elevation may bias the amplitude and shape of the temperature changes inferred from $\delta^{18}O_{ice}$ (Dahl-Jensen et al. 1998; Lang et al. 1999; Severinghaus and Brook 1999; Landais et al. 2004b, c). Comparisons of various paleothermometry methods have clearly shown that the apparent $\delta^{18}O_{ice}$-temperature slope varies at all timescales.

Air isotopic measurements in ice cores (nitrogen, oxygen and argon) offer a complementary tool to the water isotopes for climatic quantitative reconstructions. First, the combination of air and water isotopic measurement permits us to distinguish between climatic variability and stratigraphic disturbances (Chappellaz et al. 1997; Landais et al. 2004a). Second, it enables an independent reconstruction of the surface temperature evolution for rapid temperature changes (Severinghaus and Brook 1999, Lang et al. 1999; Landais et al. 2004b, c). Finally, like methane concentration, the isotopic composition of atmospheric oxygen is a powerful dating tool. Both are global atmospheric tracers because of their relatively long atmospheric residence times (1,000–2,000 years for O_2 and 10 years for CH_4, compared to the 1 year interhemispheric exchange time). Consequently, identification of the same patterns of CH_4 and $\delta^{18}O$ of O_2 in two different cores enables one to produce a common timescale (Blunier et al. 1998, 2001; Bender et al. 1999; Landais et al. 2003).

We present here a high-resolution record (~50 years over DO 23 and 24) of $\delta^{15}N$, $\delta^{40}Ar$ and $\delta^{18}O$ of O_2 in the air trapped in the NorthGRIP ice core over the sequence covering the glacial inception. We first demonstrate the absence of any stratigraphic disturbance over the bottom part of the NorthGRIP core (below 2,870 m). We use the combined measurements of $\delta^{15}N$ and $\delta^{40}Ar$ to estimate the amplitude of the main temperature increases associated with DO 24 and 23. In order to link this new Greenland record to other latitudes, we then construct a common timescale of the NorthGRIP and Vostok ice isotopic profiles ($\delta^{18}O_{ice}$ and δD_{ice}, respectively). Such North–South comparison is achieved

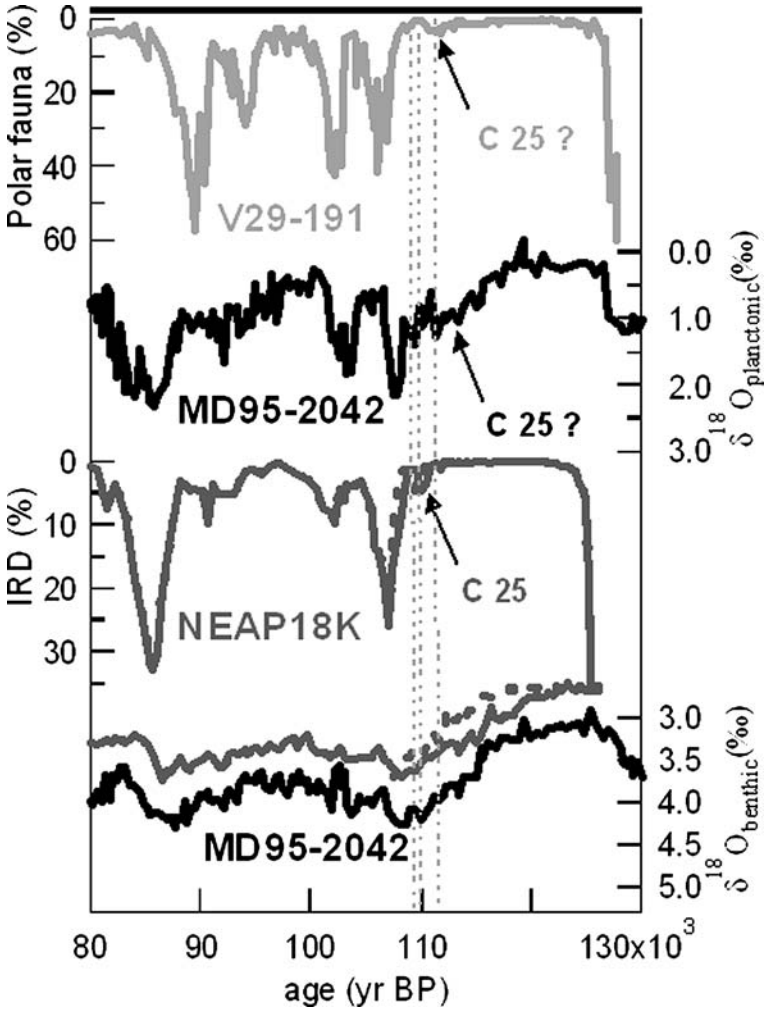

Fig. 1 *First panel* Polar fauna counts from the ODP 980 core, west of Ireland, on its own timescale (Mc Manus et al. 2002). *Second panel* $\delta^{18}O_{planktonic}$ from the MD 95-2042 core, Iberian margin, on its own timescale (Shackleton et al. 2002). *Third panel* IRD signal from the NEAP18K core, southeast of Greenland, on its own timescale (Chapman and Shackleton 1999; *dotted line*) and on the MD 95-2042 timescale after a benthic $\delta^{18}O$ correlation (*solid line*). *Fourth panel* $\delta^{18}O_{benthic}$ from the MD 95-2042 core on its own timescale (*black*), the ODP 980 core on its own timescale (*light grey*), the NEAP18K core on its own timescale (*dark grey*, *dotted line*) and after a correlation over the $\delta^{18}O_{benthic}$ increase with MD 95-2042 (*dark grey*, *solid line*)

through the use of $\delta^{18}O$ of O_2 and published methane data. Finally, from the amplitude of the rapid temperature increases and the Greenland/Antarctic phasing of events, we discuss the uniqueness of the first DO of the last glacial period.

2 Method

A total of 130 duplicate measurements of $\delta^{15}N$ and $\delta^{18}O$ were performed between 2,870 and 3,085 m depth on the air trapped in the NorthGRIP ice core. The associated uncertainty is 0.006 and 0.015‰, respectively, for $\delta^{15}N$ and $\delta^{18}O$, estimated using the pooled standard deviation over all duplicate samples. The air was extracted with a melt-refreeze method and analysed on a mass spectrometer (Finnigan MAT 252). Corrections were applied for the influence of interfering masses (Severinghaus et al. 2001). We also performed 47 measurements of $\delta^{40}Ar$ in the air from the NorthGRIP ice core corresponding to the main temperature increases associated with DO 23 and 24. The wet gas extraction was followed by the destruction of all gases except noble gases in a getter (alloy of zirconium and aluminium heated at 900°C; Severinghaus et al. 2003) to improve the analytical uncertainty (0.025‰ from the pooled standard deviation over a dozen duplicate measurements when enough ice was available).

The $\delta^{15}N$ signal is a product of thermal and gravitational fractionation in the firn (i.e. the unconsolidated snow that constitutes the upper part of the ice sheet, 70 m in NorthGRIP today). The air isotopic composition is recorded as the air becomes trapped during pore close-off at the bottom of the firn. The gravitational fractionation reflects the isotopic enrichment with depth due to the gravity field. The thermal fractionation results from transient temperature gradients in the firn that drive the heavier isotopes towards the colder end as $\delta_{therm} = \Omega\ \Delta T$ (the thermal diffusion coefficient, Ω, is specific to each isotopic pair). Because heat diffuses ten times slower through the firn than gas (Severinghaus and Brook 1999), a rapid warming/cooling at the surface of the Greenland ice sheet, which is reflected as a transient temperature gradient in the firn, leads to an enrichment/depletion of heavier isotopes at the bottom of the firn. Such positive/negative anomaly in the $\delta^{15}N$ is finally recorded in the air trapped during pore close-off (Severinghaus et al. 1998).

The properties of thermal fractionation make possible the quantification of the amplitude of rapid temperature changes. This first requires the separation of thermal and gravitational signals and, secondly, the surface temperature change has to be estimated from the transient temperature gradient in the firn. By combining measurements of $\delta^{15}N$ and $\delta^{40}Ar$ one can eliminate the gravitational signal, identical for $\delta^{15}N$ and $\delta^{40}Ar/4$ since it depends on the mass differences between both isotopes. The calculation of $\delta^{15}N_{excess} = \delta^{15}N - \delta^{40}Ar/4 = (\Omega_N - \Omega_{Ar}/4)\Delta T$ (Severinghaus and Brook 1999) then gives direct access to the temperature gradient in the firn since Ω_N and Ω_{Ar} have been precisely determined (Grachev and Severinghaus 2003a, b). Because of heat diffusion, the temperature gradient in the firn is less than the true surface temperature change. The amplitude of this change can be determined with a firnification and heat diffusion model (Goujon et al. 2003; Severinghaus and Brook 1999) independently from its duration (Landais et al. 2004b).

$\delta^{18}O$ of O_2 in air bubbles is also affected by thermal and gravitational fractionations. However, unlike nitrogen and argon, atmospheric oxygen does not have a constant isotopic composition. Its changes are driven by the extent of continental ice sheets, which influences the $\delta^{18}O$ of H_2O of the global ocean, $\delta^{18}O_{global\ ocean}$. Photosynthesis transmits these variations in oceanic isotopic composition to atmospheric oxygen, such that the variations of atmospheric $\delta^{18}O$ will indirectly reflect the $\delta^{18}O_{global\ ocean}$ variations (Sowers et al. 1991). Because the ocean signal is transmitted to the atmosphere via biological pathways, in addition to the global ice volume signal, some of the $\delta^{18}O$ of O_2 variations are linked to global biospheric productivity processes as well as H_2O and O_2 fractionations in the biosphere (e.g. Bender et al. 1994; Leuenberger 1997). The long residence time of O_2 in the atmosphere results in its becoming globally homogenized, such that, for any given time period, the $\delta^{18}O$ of O_2 recorded for the air trapped in the ice in Greenland and Antarctica should be identical (after correction for the gravitational and thermal effects and neglecting alterations during the bubble close-off process and storage). The $\delta^{18}O$ of O_2 is classically calculated as $\delta^{18}O_{atm} = \delta^{18}O - 2\delta^{15}N$ from ice cores, since the gravitational signal will affect $\delta^{18}O$ twice as much as $\delta^{15}N$. Such a definition neglects the thermal effect or implicitly assumes a thermal diffusion coefficient for oxygen, Ω_O, twice the one for nitrogen, Ω_N. Firn experiments (Severinghaus et al. 2001) gave,however,a value of 1.6 for the ratio Ω_O/Ω_N. The classical calculation consequently underestimates the $\delta^{18}O_{atm}$ during rapid temperature change (this underestimation can be up to 0.05‰ in Greenland during a strong surface temperature increase, i.e. more than 10°C in 100 years). In this study, through our determination of $\delta^{15}N_{excess}$, we can separate the thermal and gravitational signals on the DO 23 and 24, and therefore propose an estimation of $\delta^{18}O_{atm}$ corrected for both the thermal and the gravitational signals.

3 Results

The $\delta^{15}N$ profile (Fig. 2) depicts rapid variations over DO 23 and 24. Each positive/negative anomaly depicted in the $\delta^{15}N$ profile is recorded 7–8 m deeper than a corresponding increase/decrease in $\delta^{18}O_{ice}$. This observed depth difference is in agreement with the depth difference, Δdepth, between the temperature variations recorded in the ice ($\delta^{18}O_{ice}$) and gas ($\delta^{15}N$), as obtained from the combined values of the thinning function around 2,900 m and the expected firn close-off depth (NorthGRIP community members 2004). Such $\delta^{15}N$ anomalies can therefore only be the result of thermal fractionation. The correspondence between $\delta^{18}O_{ice}$ and $\delta^{15}N$ confirms the integrity of the ice core record and that the variations in the $\delta^{18}O_{ice}$ profile are of climatic origin.

While the combination of $\delta^{15}N$ and $\delta^{18}O_{ice}$ clearly confirms that the DO 23 and 24 from the NorthGRIP bottom part are true climatic signals, limited sampling resolution prevents us from identifying whether a $\delta^{15}N$ signal is associated with DO 25 as recorded in the $\delta^{18}O_{ice}$ profile. However, highly detailed methane records performed in the new Dome C ice core clearly reveal a significant peak at the beginning of the last glacial period before the peak associated to DO 24 (Chappellaz J, personal communications). Methane variations of the last glacial period have been shown to reflect the temperature changes in the North (Chappellaz et al. 1993). As a consequence, even if our dataset does not enable us to reject the hypothesis of an ice stratigraphic perturbation, it is very likely that DO 25 is a true climatic event.

To infer the amplitude of the rapid temperature increases associated with DO 23 and 24, we calculated the $\delta^{15}N_{excess}$ from $\delta^{15}N$ and $\delta^{40}Ar$ measurements over both events. Then, we fitted our $\delta^{15}N_{excess}$ profile with a modelled $\delta^{15}N_{excess}$ obtained as output of the firnification and heat diffusion model by Goujon et al. (2003) (Fig. 2, details of the method are in Landais et al. 2004b). The best fit was obtained with temperature increases of 10 ± 2.5 and 16 ± 2.5°C, respectively, for DO 23 and 24. In this estimate, no correction was applied for gas loss that affects the $\delta^{40}Ar$ (Severinghaus et al. 2003) since our $\delta O_2/N_2$ record (not shown) shows neither significant variations over DO 23 and 24 (< 2‰) nor important gas loss (the samples were analysed between 6 and 18 months after drilling). The 16°C temperature increase associated with DO 24 is similar to that obtained for DO 19 both in GRIP and NorthGRIP with similar methods (Lang et al. 1999; Landais et al. 2004c). DO 19 depicts the largest rapid $\delta^{18}O_{ice}$ variation associated with a DO over the last glacial period. This makes it most probably one of the largest DO in terms of associated Greenland surface temperature change. In this respect, DO 24 fits the profile of a "classical" DO even if its associated $\delta^{18}O_{ice}$ variation suggests smaller amplitude for the temperature increase.

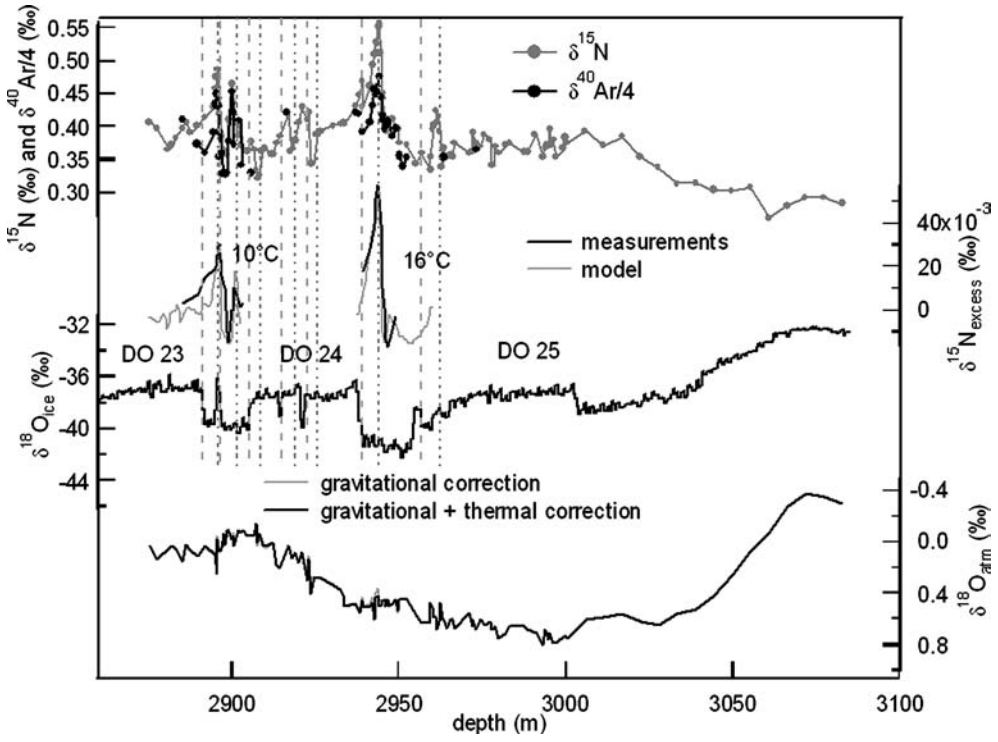

Fig. 2 *First panel* $\delta^{15}N$ (*grey*) and $\delta^{40}Ar$ (*black*) measurements. *Second panel* $\delta^{15}N_{excess}$ calculated from $\delta^{15}N$ and $\delta^{40}Ar$ measurements (running mean over three points). *Third panel* $\delta^{18}O_{ice}$ (NorthGRIP community members 2004). *Fourth panel* $\delta^{18}O_{atm}$ corrected for gravity only ($\delta^{18}O_{atm} = \delta^{18}O - 2\,\delta^{15}N$, *grey line*) and for thermal and gravitational fractionations [$\delta^{18}O_{atm} = \delta^{18}O - 2\,(1-f)\,\delta^{15}N - 1.6\,f\,\delta^{15}N$ with f being the thermal signal fraction of the total signal, calculated as $f = (\delta^{15}N_{excess}/\delta^{15}N)\,(\Omega_{N}/(\Omega_{N} - \Omega_{Ar}/4))$, *black line*]. This second-order correction is almost negligible. The *dashed* and *dotted grey* lines help to locate the rapid events recorded, respectively, in the ice and in the gas records. NB: Three $\delta^{40}Ar$ points measured around 2,950 m depict a slight 0.05‰ variation while the two closest $\delta^{15}N$ points show no variation. At that depth, $\delta^{40}Ar$ and $\delta^{15}N$ were not measured on the same samples to save ice and to allow the quantification of the reproducibility of $\delta^{40}Ar$ measurements. We cannot therefore conclude as to the origin of this variation, whether it is climatic or linked to our measurements ($\sigma = 0.025$‰ for $\delta^{40}Ar$ and $\sigma = 0.006$‰ for $\delta^{15}N$). Note, however, in support of our temperature quantification that no rapid variations of $\delta^{15}N$ and $\delta^{40}Ar$ were evidenced during periods of stable surface temperature (Landais et al. 2004b, c). The choice of a baseline before the rapid temperature increase to calculate the amplitude of temperature change was discussed in a previous methodology paper (Landais et al. 2004b)

We next compare the glacial inception in Greenland and Antarctica by synchronizing the timescales using $\delta^{18}O$ of O_2. Our $\delta^{18}O_{atm}$ measurements for NorthGRIP (Fig. 2) show a smooth evolution, in contrast to the rapid $\delta^{18}O_{atm}$ excursions observed in the bottom part of GRIP (Fuchs and Leuenberger 1996; Chappellaz et al. 1997; Landais et al. 2003), confirming that the ice stratigraphy should be preserved in the whole NorthGRIP bottom part. The correction for thermal fractionation in addition to the gravitational fractionation does not significantly modify the $\delta^{18}O_{atm}$ profile (Fig. 2). Note that no correction for gas loss was considered for the $\delta^{18}O_{atm}$ since the $\delta O_2/N_2$ values remain around −10‰, i.e. significantly less than the −30‰ observed for badly preserved ice (Landais et al. 2003). The $\delta^{18}O_{atm}$ increases from −0.4‰ at the greatest depth to +0.8‰ (2,990 m), then decreases to −0.1‰ (2,900 m). This profile parallels the Antarctic Vostok $\delta^{18}O_{atm}$ record (Sowers et al. 1993) over the glacial inception (Fig. 3). The $\delta^{18}O_{atm}$ minimum around −0.4‰ at the bottom of the NorthGRIP ice core corresponds to full interglacial conditions in Vostok. From this we conclude that the bottom of the NorthGRIP core is 120–123 kyears BP, according to the Vostok GT4 timescale (Petit et al. 1999).

Extending the correlation over the entire glacial inception requires choosing $\delta^{18}O_{atm}$ tie points. As a consequence of the long residence time of oxygen in the atmosphere, $\delta^{18}O$ of O_2 varies slowly, making the choice of correlation points between both profiles subject to some uncertainty. An additional correlation constraint is provided by the rapid increase in methane concentration associated with DO 24 that is recorded both in NorthGRIP (NorthGRIP community member 2004) and in Vostok (Caillon et al. 2003a). Taking the Vostok GT4 timescale as a reference, the identification of the rapid methane increase in both cores gives an age of 105.3 kyears BP to the NorthGRIP gas at 2,944.20 m depth. Finally, from the $\delta^{18}O_{atm}$ and CH_4 constraints, we propose a relative dating of the 200 deepest meters of the NorthGRIP ice core with respect to Vostok. We applied the following procedure:

1. The Vostok and NorthGRIP $\delta^{18}O_{atm}$ curves are matched using five tie points (maxima, minima and

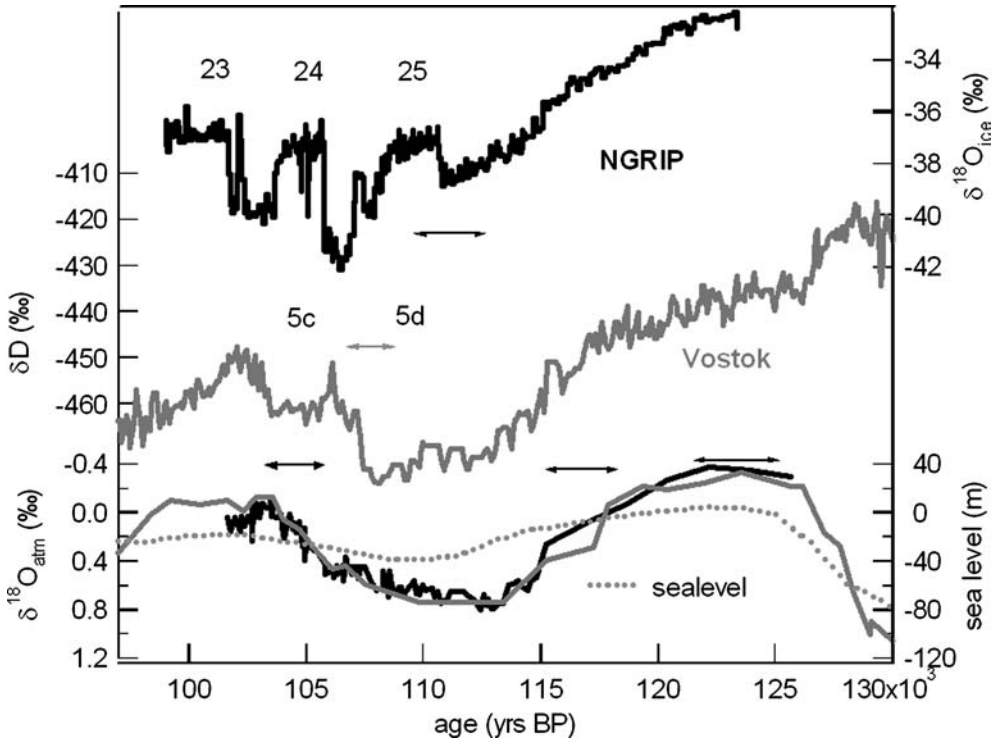

Fig. 3 *Top* $\delta^{18}O_{ice}$ evolution in NorthGRIP on the Vostok GT4 age scale (NorthGRIP community members 2004). The *horizontal arrows* represent the combined uncertainty linked to the NorthGRIP/Vostok $\delta^{18}O_{atm}$ correlation and to the NorthGRIP Δage. *Middle* δD evolution in Vostok on the GT4 timescale (Petit et al. 1999). The *horizontal arrow* indicates the uncertainty on the Vostok Δage. *Bottom* $\delta^{18}O_{atm}$ used for the Vostok/NorthGRIP correlation on GT4 timescale superimposed to the sea-level curve inferred by Waelbroeck et al. (2002) on its own timescale. The *horizontal arrows* indicate the uncertainty in the $\delta^{18}O_{atm}$ correlation between Vostok and NorthGRIP (see text). NB: The $\delta^{18}O_{atm}$ values are from Petit et al. (1999) and were only corrected for gravitational fractionation. The total uncertainty should be calculated by taking into account both the uncertainty from the first panel ($\delta^{18}O_{atm}$ correlation + Δage in NorthGRIP) and the uncertainty from the middle panel (Δage in Vostok). The resulting uncertainty is maximal for the greatest depths and was estimated to be ±2,500 years

mid-slopes of the $\delta^{18}O_{atm}$ profiles, 20 different point identifications were tried).

2. A timescale for the NorthGRIP $\delta^{18}O_{atm}$ profile is obtained by using a linear interpolation of the depth levels over the five tie points linking NorthGRIP depth and Vostok GT4 age. We prefer a linear interpolation to a function integrating the small effect of thinning and accumulation rate between two nearby tie points. Indeed, the thinning is reduced over the bottom part of the NorthGRIP ice core due to the high rate of basal ice melting (NorthGRIP community members 2004). Moreover, the estimate of the accumulation rate variations over the glacial inception from the water isotopes profile alone is not straightforward because of the huge changes of the hydrological cycle. Sensitivity tests show that these influences will not modify our chronology given the associated error bars. An ongoing project for dating the whole NorthGRIP ice core using a glaciological model will permit better constraints on accumulation rate and thinning.
3. The resulting timescale gives an age for the depth of the rapid methane increase (2,944.20 m).
4. The area between both mean-centred $\delta^{18}O_{atm}$ profiles on the Vostok GT4 timescale is minimized and we did not authorize a difference superior to 600 years (i.e. the NorthGRIP methane profile resolution) between the NorthGRIP gas age at 2,944.20 m and 105.3 kyears BP (age of the rapid methane increase on the Vostok GT4 timescale).

The error bars for this correlation remain subjective: they correspond roughly to the maximal uncertainty on the visual choice of the $\delta^{18}O_{atm}$ tie points. On a more objective way, we have decided to reject the correlation when the area between the two $\delta^{18}O_{atm}$ profiles was four times the area corresponding to the best correlation. A more constrained North–South correlation, with clearer tie points, will be available when detailed methane measurements will be performed over the whole bottom part of the NorthGRIP ice core.

The second step in describing the North–South sequence over the glacial inception is to compare the Vostok δD and NorthGRIP $\delta^{18}O_{ice}$ profiles on the same ice timescale. Since the common timescale developed above is for the gases in each core, transferring the chronology to ice requires knowing the Δage between ice and gas ages over the period of

interest. For Vostok, the modelled Δage estimate of the GT4 timescale over this period has an associated uncertainty of 1,000 years (Petit et al. 1999). Using $\delta^{15}N$ and $\delta^{40}Ar$ measurements, Caillon et al. (2001) confirmed the value of the modelled Δage (5,000 years) around 108 kyears BP in Vostok. Furthermore, a recently refined ice and gas timescale for Vostok (Parrenin et al. 2004) only slightly modifies the Δage over that period. We therefore use the GT4 Δage and retain a Δage uncertainty of 1,000 years for the Vostok ice timescale (Fig. 3, middle). For NorthGRIP, the Δage can be calculated using the firnification and heat diffusion model of Goujon et al. (2003): it varies between 300 and 600 years depending on the surface conditions (accumulation rate, temperature). The associated uncertainty is around 100 years (10% of Δage). Such a small uncertainty is supported by Fig. 2 where the modelled $\delta^{15}N_{excess}$ variations coincide with the measured $\delta^{15}N_{excess}$ ones on the same depth scale, therefore validating the use of the model for Greenland studies even if problems remain for Vostok applications (Goujon et al. 2003).

In summary, the NorthGRIP $\delta^{18}O_{ice}$ and Vostok δD profiles can be compared on the same GT4 timescale (Fig. 3). The age uncertainty for the NorthGRIP $\delta^{18}O_{ice}$ profile results from the combination of three sources of errors:

1. The $\delta^{18}O_{atm}$ correlation
2. The Δage
3. The GT4 age

Only the first two errors are relevant to the following discussion of the relative evolution of surface temperature between Greenland and Antarctica over the glacial inception.

Even if the uncertainties in the NorthGRIP/Vostok relative dating are large (up to 2,500 years), the δD and $\delta^{18}O_{ice}$ profiles clearly show that the temperature increase associated with DO 25 occurs at a time when the Vostok temperature is at a relative minimum. The following Antarctic temperature increase associated with the 5d/5c transition in the Vostok δD profile seems to precede the rapid temperature increase of DO 24. We are quite confident in this result since the onset of DO 24 is strongly cross-dated by the methane tie point. Moreover, such a result was already pointed out in Caillon et al. (2003a) who extended the North–South climatic asynchrony described by Blunier et al. (2001) to the beginning of the last glacial. The same pattern is suggested for DO 23; however, we hesitate to draw a firm conclusion in this case because of the large uncertainty in the relative timescale and the absence of detailed methane data to provide a strong tie point between Vostok and NorthGRIP for this time period. As opposed to DO 23 and 24, DO 25 has no Antarctic counterpart and therefore appears to be an exception to the proposed North/South seesaw mechanism (Stocker and Johnsen 2003).

The rapid temperature increase associated with the DO 25 marks the onset of the rapid climatic variability in the North Atlantic. Before this event, the NorthGRIP $\delta^{18}O_{ice}$ and Vostok δD profiles first show a common cooling during 10 kyears. The phasing, however, cannot be firmly established because of the ±2,500 years uncertainty in the relative timescales. Moreover, this relationship can be challenged since the interpretation of ice isotopic profiles in terms of surface temperature is not straightforward, especially during strong modifications of the water cycle. Cuffey and Vimeux (2001) showed that accounting for the temperature of the evaporative regions through combined measurements of δD and $\delta^{18}O$ in the ice and for the isotopic composition of the global ocean leads to a corrected Vostok surface temperature over the glacial inception (i.e. not proportional to the δD of the ice). Using that temperature reconstruction, the Antarctic cooling is slightly delayed and suggests that the main Antarctic temperature decrease occurred only 2–3 kyears after the main Greenland temperature decrease (Fig. 4), which still lies within our uncertainty range. We performed preliminary measurements of δD over the bottom part of the NorthGRIP core to apply the same temperature reconstruction method as Cuffey and Vimeux (2001) and Masson-Delmotte et al. (2005b) from combined measurements of δD and $\delta^{18}O$ of the ice. Such a reconstructed surface temperature profile is parallel to the $\delta^{18}O_{ice}$ one, supporting our aforementioned conclusion.

To strengthen our description of the North–South relationship over the glacial inception, we point out that the NorthGRIP ice core is not the only Greenland core to contain ice over this period. In the Summit GRIP ice core, a discontinuous reconstruction of the $\delta^{18}O_{ice}$ profile on the Vostok GT4 timescale was obtained (through a methane/$\delta^{18}O_{atm}$ correlation; Landais et al. 2003), which can be compared to the NorthGRIP glacial inception $\delta^{18}O_{ice}$ profile (Fig. 4). Within the limits of the timescale uncertainty, both GRIP and NorthGRIP $\delta^{18}O_{ice}$ profiles show similar timing for the glacial inception in Greenland. The δD profile has also been measured on the bottom part of the GRIP ice core (Jouzel et al. 2005). The surface temperature profile was reconstructed following Cuffey and Vimeux (2001) (Fig. 3; Jouzel et al. in press) and yielded a profile that parallels the $\delta^{18}O_{ice}$, as we found for NorthGRIP. Finally, given the cross-dated profiles of NorthGRIP, GRIP and Vostok ice isotopic measurements and GRIP and Vostok temperature reconstructions, we conclude that the significant progressive cooling corresponding to the glacial inception is roughly in phase between Greenland and Antarctica. Again, this conclusion could be further refined as more dating constraints become available from the NorthGRIP methane profile.

While temperature appears to decrease in parallel over both poles, it is interesting to underline the timing of CO_2 decrease (Fig. 4; Barnola et al. 1987). While the CO_2 concentration remains high during the slow polar tem-

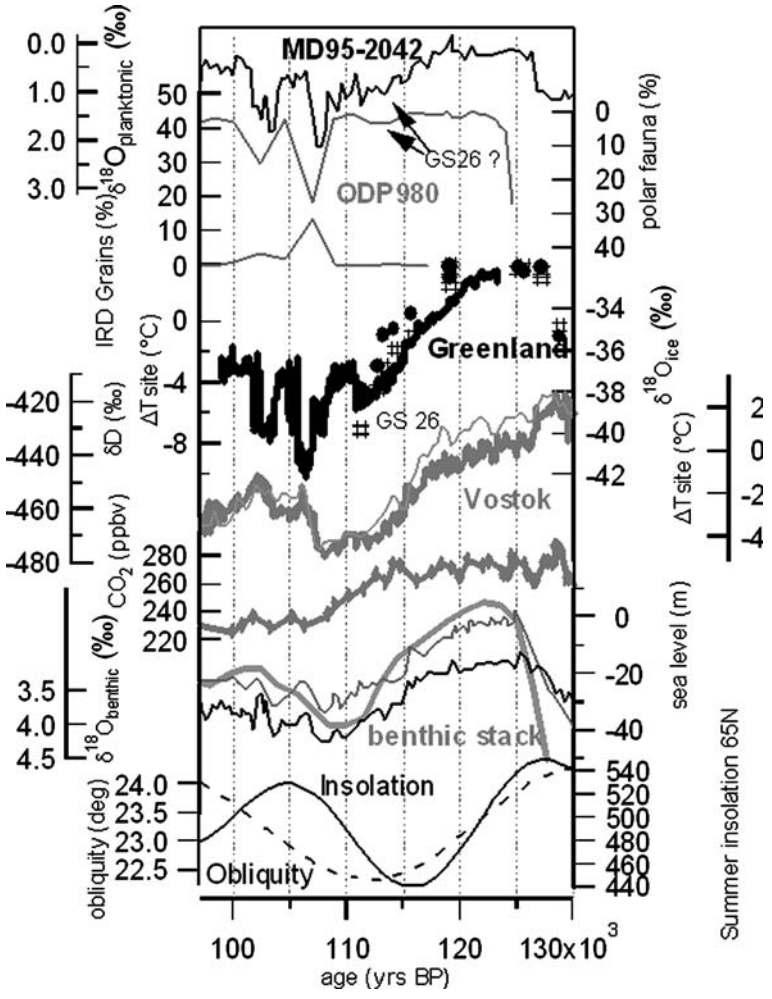

Fig. 4 Sequence for the glacial inception on the GT4 timescale (except for marine records). *From top to bottom* (1) planktonic $\delta^{18}O$ for the marine core MD 95-2042, Iberian margin, on its own timescale (Shackleton et al. 2002). (2) Polar fauna from the marine core ODP 980, west of Ireland, on its own timescale (Mc Manus et al. 2002). (3) IRD signal from the marine core ODP 980 (Mc Manus et al. 2002) on its own timescale. (4) $\delta^{18}O_{ice}$ for the glacial inception in NorthGRIP (*black continuous line*) and in GRIP (*filled circles*). The *pounds* indicate the surface temperature reconstructed in GRIP from δD, $\delta^{18}O$ and $\delta^{18}O_{global\ ocean}$. The temperature variations are expressed relative to the present mean annual surface temperature in GRIP. (5) δD for the glacial inception in Vostok (Petit et al. 1999; *thick line*) and reconstructed surface temperature (Cuffey and Vimeux 2001; *thin line*). Variations of temperature are expressed relative to the present mean annual surface temperature at Vostok. (6) CO_2 evolution from the Vostok ice core (Barnola et al. 1987). (7) Sea-level curve (Waelbroeck et al. 2002), $\delta^{18}O_{benthic}$ from ODP 980 (Mc Manus et al. 2002) and $\delta^{18}O_{benthic}$ from MD 95-2042 (Shackleton et al. 2002). (8) Obliquity and 65°N summer insolation

perature decrease, the following rapid temperature increase associated with the DO 25 occurs during a period of a large CO_2 decrease. Such a CO_2 concentration decrease is clearly not causing the global cooling, which is more probably initiated by a decrease in the northern summer insolation amplified by the growing northern hemisphere ice sheets' albedo effect (Fig. 4; Berger et al. 1996; Khodri et al. 2001, 2003). Such an ice sheets' growth, mainly due to the Laurentide ice sheet with a possible contribution of the Fennoscandian ice sheet (Wang and Misak 2002; Kageyama et al. 2004), was obtained from a stack of benthic isotopic ratios after regressions between relative sea-level data and benthic foraminifers' oxygen ratios were performed in the North Atlantic and Equatorial Pacific Ocean (Waelbroeck et al. 2002). This sea-level curve depicted on Fig. 4 cannot be easily drawn on the GT4 timescale because the initial information is carried by sediment cores. However, the sea-level evolution proposed on Figs. 3 and 4 on its own timescale (Waelbroeck et al. 2002 following Martinson et al. 1987) is roughly consistent with the ice core water isotope records on the GT4 timescale. There are at least two main reasons for this:

– The northern hemisphere sediment cores indicate that the relative maximum in ice sheet volume, as inferred from $\delta^{18}O_{benthic}$, occurred during the warm phase of DO 25 (Shackleton et al. 2002). The same pattern also appears in Figs. 3 and 4, where the warm phase of DO 25 in NorthGRIP coincides with the maximum in $\delta^{18}O_{global\ ocean}$.

– As for the sea-level curve, the NGRIP $\delta^{18}O_{atm}$ profile on the GT4 timescale, partly linked to ice sheets' volume, shows a clear maximum during the warm phase of DO 25. $\delta^{18}O_{atm}$ does, however, not only reflect variations in $\delta^{18}O_{global\ ocean}$ but Pépin et al. (2001) also proposed a sea-level reconstruction on the GT4 timescale on the basis of $\delta^{18}O_{atm}$ measurements corrected for biospheric effects. This reconstruction is in agreement with the one by Waelbroeck et al. (2002) over the glacial inception and shows that the minimum in $\delta^{18}O_{atm}$ roughly corresponds to the minimum in $\delta^{18}O_{global\ ocean}$.

Finally, note that we have avoided matching the $\delta^{18}O_{atm}$ with the sea-level curves because of the biosphere effects that influence the $\delta^{18}O_{atm}$ in addition to sea-level changes. Especially during the glacial inception, the importance of these other effects is illustrated by the range of $\delta^{18}O_{atm}$ variations that is two times larger than the change in $\delta^{18}O_{global\ ocean}$.

We complete our description of the glacial inception by comparing our Greenland/Antarctica sequence with high-resolution marine records from the North Atlantic (ODP 980; Mc Manus et al. 2002) and the Iberian margin (MD 95-2042; Shackleton et al. 2002). We have kept the original marine cores' timescales because of the aforementioned good agreement between the GT4 and the marine timescales over the glacial inception, and because the sea surface temperature records ($\delta^{18}O_{planktonic}$ and polar fauna percentages) depict parallel evolution to the NorthGRIP $\delta^{18}O_{ice}$ (Fig. 4). From this, we can establish a tentative comparison of the ice core records on the GT4 timescale with the two marine records over the glacial inception. This comparison suggests that the cold phase GS 26 (before the DO 25 warm phase) manifested itself in the northern Atlantic region as well as in the mid-latitude surface ocean (up to the Iberian margin, MD 95-2042) as a slight cooling (less than one-fourth of a typical rapid cooling during the last glacial). No clear IRD signal is recorded, except the one found by Chapman and Shackleton (1999), which seems to occur during the warm phase of DO 25 (Shackleton et al. 2002), suggesting that GS 26 was not driven by an iceberg discharge (Fig. 1). Summarizing, the sequence for the glacial inception and the beginning of the glacial period is the following:

– The polar temperature decreases in both the North and the South. The slow growth of ice sheets seems to be in phase with or slightly lags the polar temperature decrease, as described by Cortijo et al. (1994, 1999). This ice sheet growth was probably driven by the summer temperature decrease at polar latitudes (Oerlemans 2001) as a consequence of the decreased northern insolation. The obliquity decrease acts as a positive feedback for the ice sheet growth because of the associated increase in low- and high-latitude insolation gradients that enhances the transport of water masses (Fig. 4; Ruddiman and McIntyre 1979; Khodri et al. 2001). The CO_2 level stays high during this first stage of high-latitude cooling.
– The first rapid event (succession of GS 26 and DO 25) is recorded in the northern hemisphere but has no Antarctic counterpart. It is triggered while the CO_2 level and ice sheet size are still intermediate between interglacial and full glacial values. The increased precipitation, already invoked for the rapid ice sheet growth, could be involved in the onset of such an event since no clear IRD peak is recorded in sediment cores. We propose that the intense thermohaline circulation (THC) during the growth of the polar ice sheets over the glacial inception can suddenly become unstable because of a too high fresh water input from increased precipitation over the ocean. Such rapid instability of the THC at the end of the interglacial is suggested by marine indicators (Adkins et al. 1997; Mc Manus et al. 2002).
– During the warm phase of DO 25 and the preceding GS 26, the ice sheets' volume reached a relative maximum and the atmospheric CO_2 shows its first large decrease. We suggest that the general cooling of the polar oceans, depicted by the marine and ice cores' records, acts as a CO_2 pump (the southern ocean probably has an important role here, as suggested previously, e.g. Petit et al. 1999). The role of vegetation on the CO_2 evolution should also be considered, but seems to be of minor importance since, over DO 25, vegetation over Europe did not significantly differ from its interglacial state (Reille et al. 1998; Sanchez-Goñi et al. 1999; Rioual et al. 2001).
– After the warm phase of DO 25, the CO_2 level is intermediate between glacial and interglacial levels and DO 24 and 23 show the major characteristics of "classical" DO (temperature change amplitude, southern hemisphere reaction, IRD signals).

Additional high-frequency temperature changes appear to affect Greenland during the sequence of DO 23 and 24 with surprising rapid coolings during the warm phase of DO 24. We estimate that the mean period for the succession of two rapid temperature increases or decreases over that period is 800 years, taking into account all the rapid $\delta^{18}O_{ice}$ variations of more than 1‰ amplitude in less than 200 years. By comparison, doing the same exercise over the full glacial period gives a mean periodicity of 1,500 years. Such a very rapid climatic variability, with additional rapid events occurring between the classically defined DO, has only one equivalent during the last glacial period: the beginning of Marine Isotopic Stage 3 (−55 to −60 kyears). This latter period is characterized by a sea level (or ice sheet size) close to the one estimated over the sequence of DO 23 and 24 (Shackleton 1987; Waelbroeck et al. 2002). It suggests a relative instability of the THC and rapid switches between active and "off" modes, as already pointed out by Adkins et al. (1997). Indeed, following the classical interpretation of the succession of DO (Ganopolski et al. 2001), the cold phases over Greenland are associated with reduced THC activity or

southern deep water convection, while the warm phases are associated with an active THC or northern deep water convection that brings heat towards northern latitudes. Except for the GS 25 preceding DO 24 and a slight signal for the GS 24 before DO 23, the short cold phases are not associated with clear IRD signals in the marine cores. As for the onset of GS 26 and DO 25, we propose again that the hydrologic cycle plays a key role in switching on and off the THC with a north Atlantic freshwater threshold budget close to a critical point. Several environmental records (e.g. Sanchez-Goñi et al. 1999) and modelling studies over the glacial inception (e.g. Khodri et al. 2001) confirm that high precipitation rates over high- and mid-latitudes have characterized the whole stage 5 (~130–90 kyears BP).

Finally, our proposed sequence of events associated with the glacial inception (simultaneous cooling in north and south and moderate increase in continental ice volume, followed by the CO_2 decrease) contrasts with the somewhat different situation during glacial terminations. By comparing the Byrd (Antarctica) and GISP2 records, the Greenland warming during the last termination started slowly 2 kyears or less before the initiation of the Antarctic warming (Alley et al. 2002). Then, the Greenland main warming (Bølling-Allerød) occurred only 6 kyears after the beginning of Antarctic warming. Moreover, the analysis of the properties recorded in the Vostok and EPICA Dome C Antarctic cores indicates that during terminations: (1) the temperature at high southern latitude increases only a few hundred years before CO_2 (Monnin et al. 2001; Caillon et al. 2003b), (2) the dynamics of the warming was very different between North and South and (3) the northern ice sheet deglaciation occurred several thousand years after the southern warming (Pépin et al. 2001).

4 Conclusion

We have used air isotopic measurements in the NorthGRIP ice core to confirm the large climatic variability during the glacial inception and to estimate the amplitude of the temperature changes associated with DO 23 and 24. In addition, we propose a relative dating of the Greenland glacial inception with respect to East Antarctic temperature, atmospheric CO_2 evolution and global ice sheet growth. According to this dating, the glacial inception involved synchronous cooling at both poles during the initial slow growth of the northern hemisphere ice sheets. Rapid climatic variability in the North Atlantic initiated with DO 25, which seems to be associated with a small temperature change and has no Antarctic counterpart. It occurred before ice sheets reached their glacial maximum extent and while atmospheric CO_2 was still relatively elevated. After that event, atmospheric CO_2 dropped to glacial levels and NorthGRIP DO 24 and 23 depict characteristics of classical DO (up to +16°C for DO 24, i.e. comparable to the DO 19 at the same site; IRD signal; Antarctic counterpart). Finally, the rapid climatic variability during the warm and cold phases of DO 23 and 24 suggests that the THC encountered frequent shifts between "off" and "on" modes. The first rapid event, DO 25, which occurred during the initial ice sheet build-up, suggests a key role for the atmospheric hydrological cycle in climate dynamics. The water cycle influence has already been proved to favour the glacial inception. We show here that it could additionally create a rapid climatic variability when the influence of ice sheets discharge is reduced.

Acknowledgments This work was supported by the EC within the POP project (EVK2-2000-22067), the CEA, the French CNRS, the Balzan foundation and the IPEV. It is a contribution to the North Greenland Ice Core Project (NGRIP) organized by the ESF. The comments of the reviewers strongly helped to improve the manuscript. We appreciated fruitful discussions with J. Chappellaz and J.-M. Barnola. We thank G.B. Dreyfus and H. Blatt for their help on the manuscript and all NorthGRIP participants for their cooperative effort.

References

Adkins JF, Boyle EA, Keigwin L, Cortijo E (1997) Variability of the North Atlantic thermohaline circulation during the last interglacial period. Nature 390:154–156

Alley RB, Brook EJ, Anandakrishnan S (2002) A northern lead in the orbital band: north–south phasing of Ice-Age events. Q Sci Rev 21:431–441

Barnola JM, Raynaud D, Korotkevich YS, Lorius C (1987) Vostok ice core provides 160,000-year record of atmospheric CO_2. Nature 329:408–414

Bender M, Sowers T, Labeyrie LD (1994) The Dole effect and its variation during the last 130,000 years as measured in the Vostok core. Glob Biog Cycles 8(3):363–376

Bender M, Malaize B, Orchado J, Sowers T, Jouzel J (1999) High precision correlations of Greenland and Antarctic ice core records over the last 100 kyr. In: AGU (eds) Mechanisms of global climate change at millennial time scales. Geophysical Monograph series, pp 149–164

Berger A, Gallée H, Li XS, Dutrieux A, Loutre MF (1996) Ice-sheet growth and high-latitudes sea-surface temperature. Climate Dynam 12:441–448

Blunier T, Brook EJ (2001) Timing of Millennial-scale climate change in Antarctica and Greenland during the last glacial period. Science 291(5501):109–112

Blunier T, Chappellaz J, Schwander J, Dallenbach A, Stauffer B, Stocker T, Raynaud D, Jouzel J, Clausen HB, Hammer CU, Johnsen SJ (1998) Asynchrony of Antarctic and Greenland climate change during the last glacial period. Nature 394:739–743

Bond G, Broecker W, Johnsen S, Mc Manus J, Labeyrie L, Jouzel J, Bonani G (1993) Correlations between climate records from North Atlantic sediments and Greenland ice. Nature 365:143–147

Boyle EA (1997) Cool tropical temperatures shift the global d18O–T relationship: an explanation for the ice core $\delta^{18}O$-borehole thermometry conflict. Geophys Res Lett 24:273–276

Broecker WS (1998) Paleocean circulation during the last deglaciation: a bipolar seesaw? Paleoceanography 13:119–121

Caillon N, Severinghaus J, Barnola JM, Chappellaz J, Jouzel J, Parrenin F (2001) Estimation of temperature change and gas age–ice age difference, 108 Kyr BP, at Vostok, Antarctica. J Geophys Res 106(D23):31893–31901

Caillon N, Jouzel J, Severinghaus JP, Chappellaz J, Blunier T (2003a) A novel method to study the phase relationship between Antarctic and Greenland climates. Geophys Res Lett 30(17). DOI: 10.1029/2003GL017838

Caillon N, Severinghaus JP, Jouzel J, Barnola J-M, Kang J, Lipenkov VY (2003b) Timing of Atmospheric CO_2 and Antarctic temperature changes across termination III. Science 299:1728–1731

Chapman MR, Shackleton NJ (1999) Global ice-volume fluctuation, North Atlantic ice-rafting events, and deep-ocean circulation changes between 130 and 70 ka. Geology 27:795–798

Chappellaz J, Blunier T et al (1993) Synchronous changes in atmospheric CH_4 and Greenland climate between 40 and 8 kyr BP. Nature 366:443–445

Chappellaz J, Brook E, Blunier T, Malaizé B (1997) CH_4 and $\delta^{18}O$ of O_2 records from Greenland ice: a clue for stratigraphic disturbance in the bottom part of the Greenland Ice Core Project and the Greenland Ice Sheet Project 2 ice-cores. J Geophys Res 102(C12):26547–26557

Cortijo E, Duplessy JC, Labeyrie L, Leclaire H, Duprat J, van Weering T (1994) Eemian cooling in the Norwegian Sea and North Atlantic ocean preceding continental ice-sheet growth. Nature 372:446–449

Cortijo E, Lehman S, Keigwin L, Chapman M, Paillard D, Labeyrie L (1999) Changes in meridional temperature and salinity gradients in the North Atlantic Ocean (30°–72°N) during the last interglacial period. Paleoceanography 14(1):23–33

Cuffey KM, Vimeux F (2001) Covariation of carbon dioxide and temperature from the Vostok ice core after deuterium-excess correction. Nature 412:523–527

Dahl-Jensen D, Mosegaard K, Gunderstrup GD, Clow GD, Johnsen SJ, Hansen AW, Balling N (1998) Past temperatures directly from the Greenland ice sheet. Science 282:268–271

Dansgaard W (1964) Stable isotopes in precipitation. Tellus 16:436–468

Dansgaard W, Johnsen S, Clausen HB, Dahl-Jensen D, Gundestrup N, Hammer CU, Oeschger H (1984) North Atlantic climatic oscillations revealed by deep Greenland ice cores. In: Hansen JE, Takahashi T (eds) Climate processes and climate sensitivity. Am Geophys Union, pp 288–298

Dansgaard W, Johnsen SJ, Clausen HB, Dahl-Jensen D, Gunderstrup NS, Hammer CU, Steffensen JP, Sveinbjornsdottir A, Jouzel J, Bond G (1993) Evidence for general instability of past climate from a 250-kyr ice-core record. Nature 364:218–220

Fawcett PJ, Agutsdottir AM, Alley RB, Shuman CA (1997) The Younger Dryas termination and North Atlantic deepwater formation: insights from climate model simulations and Greenland ice core data. Paleoceanography 12(1):23–38

Fuchs A, Leuenberger MC (1996) $\delta^{18}O$ of atmospheric oxygen measured on the GRIP ice core document stratigraphic disturbances in the lowest 10% of the core. Geophys Res Lett 23(9):1049–1052

Ganopolski A, Rahmstorf S (2001) Rapid changes of glacial climate simulated in a coupled climate model. Nature 409:153–158

Genty D, Blamart D, Ouahdi R, Gilmour M, Baker A, Jouzel J, Van-Exter S (2003) Precise timing of Dansgaard–Oeschger climate oscillations in western Europe from stalagmite data. Nature 421:833–837

Goujon C, Barnola J-M, Ritz C (2003) Modeling the densification of polar firn including heat diffusion: application to close-off characteristics and gas isotopic fractionation for Antarctica and Greenland sites. J Geophys Res 108(D24). DOI: 10.1029/2002JD003319

Grachev AM, Severinghaus JP (2003a) Determining the thermal diffusion factor for $^{40}Ar/^{36}Ar$ in air to aid paleoreconstruction of abrupt climate change. J Phys Chem 107(A2003):4636–4642

Grachev AM, Severinghaus JP (2003b) Laboratory determination of thermal diffusion constants for $^{29}N_2/^{28}N_2$ in air at temperature from −60 to 0°C for reconstruction of magnitudes of abrupt climatic changes using the ice core fossil-air paleothermometer. Geochim Cosmochim Acta 67(3):345–360

Grootes PM, Stuiver M, White JWC, Johnsen SJ, Jouzel J (1993) Comparison of the oxygen isotope records from the GISP2 and GRIP Greenland ice cores. Nature 366:552–554

Jouzel J, Masson-Delmotte V, Stiévenard M, Landais A, Vimeux F, Johnsen SJ, Sveinbjornsdottir AEI, White JWC (2005) Rapid deuterium-excess changes in Greenland ice cores: a link between the ocean and the atmosphere. Comptes-Rendus à l'Académie des Sciences, in press

Kageyama M, Charbit S, Ritz C, Khodri M, Ramstein G (2004) Quantifying ice-sheet feedbacks during the last glacial inception. Geophys Res Lett 31:DOI. 10.1029/2004GL021339

Khodri M, Leclainche Y, Ramstein G, Braconnot P, Marti O, Cortijo E (2001) Simulating the amplification of orbital forcing by ocean feedbacks in the last glaciation. Nature 410(6828):570–574

Khodri M, Ramstein G, Paillard D, Duplessy JC, Kageyama M, Ganopolski A (2003) Modelling the climate evolution from the last interglacial to the start of the last glaciation: the role of Arctic Ocean freshwater budget. Geophys Res Lett 30(12). DOI: 10.1029/2003GL017108

Krinner G, Genthon C, Jouzel J (1997) GCM analysis of local influences on ice core d signals. Geophys Res Lett 24(22):2825–2828

Kukla GJ, Bender M, Beaulieu de J-L, Bond G, Broecker WS, Cleveringa P, Gavin JE, Herbert TD, Imbrie J, Jouzel J, Keigwin LD, Knudsen K-L, Mc Manus JF, Merkt J, Muhs J, Muller H (2002) Last interglacial climates. Quaternary Res 58:2–13

Landais A, Chappellaz J, Delmotte MJ, Jouzel J, Blunier T, Bourg C, Caillon C, Cherrier S, Malaizé B, Masson-Delmotte V, Raynaud D, Schwander J, Steffensen JP (2003) A tentative reconstruction of the last interglacial and glacial inception in Greenland based on new gas measurements in the Greenland Ice Core Project (GRIP) ice core. J Geophys Res 108(D18). DOI: 10.1029/2002JD003147

Landais A, Steffensen JP, Caillon N, Jouzel J, Masson-Delmotte V, Schwander J (2004a) Evidence for stratigraphic distortion in the Greenland Ice Core Project (GRIP) ice core during Event 5e1 (120 kyr BP) from gas isotopes: J Geophys Res 109: doi 10.1029/2003JD004193

Landais A, Caillon N, Jouzel J, Chappellaz J, Grachev A, Goujon C, Barnola JM, Leuenberger M (2004b) A method for precise quantification of temperature change and phasing between temperature and methane increases through gas measurements on Dansgaard–Oeschger event 12 (−45 kyr). Earth Planet Sci Lett 225:221–232

Landais A, Barnola J-M, Masson-Delmotte V, Jouzel J, Chappellaz J, Caillon N, Huber C, Leuenberger M, Johnsen S (2004c) A continuous record of temperature evolution over a whole sequence of Dansgaard–Oeschger during Marine Isotopic Stage 4 (76 to 62 kyr BP). Geophys Res Let 31: DOI 10.1029/2004GL021193

Lang C, Leuenberger M, Schwander J, Johnsen S (1999) 16°C rapid temperature variation in central Greenland 70,000 years ago. Science 286(5441):934–937

Leuenberger M (1997) Modeling the signal transfer of seawater $\delta^{18}O$ to the $\delta^{18}O$ of atmospheric oxygen using a diagnostic box model for the terrestrial and marine biosphere. J Geophys Res 102(C12):26841–26850

Martinson DG, Pisias NG, Hays JD, Imbrie J, Moore TC, Shackleton NJ (1987) Age dating and the orbital theory of the ice ages: development of a high-resolution 0–300,000 years chronostratigraphy. Quaternary Res 27:1–30

Masson-Delmotte V, Jouzel J, Landais A, Stievenard M, Johnsen S, White JWC, Werner M, Sveinbjornsdottir A, Fuhrer K (2005a) Rapid and slow reorganisation of the Northern Hemisphere hydrological cycle during the last glacial period as derived from the GRIP ice core deuterium-excess record. Science 309:118–121

Masson-Delmotte V, Landais A, Stievenard M, Cattani O, Falourd S, Johnsen SJ, Jouzel J, Dahl-Jensen D, Sveinsbjornsdottir A, White JCW, Popp T, Fischer H (2005b) Greenland Holocene deuterium excess record: different moisture origins at GRIP and NorthGRIP? J Geophys Res 110: DOI 10.1029/2004JD005575

Mc Manus JF, Bond GC, Broecker WS, Johnsen SJ, Labeyrie L, Higgins S (1994) High-resolution climatic records from the N. Atlantic during the last interglacial. Nature 371:326–329

Mc Manus JF, Oppo DW, Keigwin LD, Cullen JL, Bond GC (2002) Thermohaline circulation and prolonged interglacial warmth in the North Atlantic. Quaternary Res 58:17–21

Monnin E, Indermuhle A, Dallenbach A, Flueckiger J, Stauffer B, Stocker TF, Raynaud D, Barnola J-M (2001) Atmospheric CO_2 concentrations over the last glacial termination. Science 291:112–114

NorthGRIP community members (2004) High resolution climate record of the northern hemisphere back to the last interglacial period. Nature 431:147–151

Oerlemans J (2001) Glaciers and Climate Change. Balkema Publishers, , Amsterdam. ISBN: 9026518137

Parrenin F, Remy F, Ritz C, Siegert MJ, Jouzel J (2004) New modelling of the Vostok ice flow line and implication for the glaciological chronology of the Vostok ice core. J Geophys Res 109: DOI: 10.1029/2004JD004561

Pépin L, Raynaud D, Barnola J-M, Loutre MF (2001) Hemispheric roles of climate forcings during glacial–interglacial transitions as deduced from the Vostok record and LLN-2Dmodel experiments. J Geophys Res 106(D23):31,885–31,892

Petit JR, Jouzel J, Raynaud D, Barkov NI, Barnola JM, Basile I, Bender M, Chappellaz J, Davis M, Delaygue G, Delmotte M, Kotlyakov VM, Lorius C, Pepin L, Ritz C, Saltzman E, Stievenard M (1999) Climate and atmospheric history of the past 420,000 years from the Vostok ice core, Antarctica. Nature 399:429–436

Reille M, Andrieu V, Beaulieu JLd, Guenet P, Goeury C (1998) A long pollen record from Lac du Bouchet, Massif Central, France, for the period ca 325 to 100 ka BP (OIS 9c to OIS 5e). Quaternary Sci Rev 17:1107–1123

Rioual P, Andrieu-Ponel V, Rietti-Shati M, Battarbee RW, de Beaulieu J-L, Cheddadi R, Reille M, Svobodove H, and Shemesh A (2001) High-resolution record of climate stability in France during the last interglacial period. Nature 413:293–296

Ruddiman WF, McIntyre A (1979) Warmth of the Subpolar North Atlantic Ocean during northern hemisphere ice-sheet growth. Science 204:173–175

Sanchez-Goñi MF, Eynaud F, Turon J-L, Shackelton NJ (1999) High resolution palynological record off the Iberian margin: direct land-sea correlation for the Last Interglacial complex. Earth Planet Sci Lett 171:123–137

Severinghaus J, Sowers T, Brook E, Alley R, Bender M (1998) Timing of abrupt climate change at the end of the Younger Dryas interval from thermally fractionated gases in polar ice. Nature 391:141–146

Severinghaus JP, Brook J (1999) Abrupt climate change at the end of the last glacial period inferred from trapped air in polar ice. Science 286(5441):930–934

Severinghaus JP, Grachev A, Battle M (2001) Thermal fractionation of air in polar firn by seasonal temperature gradients. G3: Geochemistry, Geophysics, Geosystems, 2: Paper number 2000GC000146

Severinghaus JP, Gratchev A, Luz B, Caillon N (2003) A method for precise measurement of argon 40/36 and krypton/argon ratios in trapped air in polar ice with application to past firn thickness and abrupt climate change in Greenland and at Siple Dome, Antarctica. Geochim Cosmochim Acta 67(3):325–343

Shackleton NJ (1987) Oxygen isotopes, ice volume and sea level. Quaternary Sci Rev 6:183–190

Shackelton NJ, Chapman M, Sanchez-Goñi MF, Paillard D, Lancelot Y (2002) The classic marine isotope substage 5e. Quaternary Res 58:14–16

Sowers T, Bender M, Raynaud D, Korotkevich YS, Orchado J (1991) The $\delta^{18}O$ of atmospheric O_2 from air inclusions in the Vostok ice core: timing of CO_2 and ice volume change during the penultimate deglaciation. Paleoceanography 6(6):669–696

Sowers T, Bender M, Labeyrie LD, Jouzel J, Raynaud D, Martinson D, Korotkevich YS (1993) 135 000 year Vostok—SPECMAP common temporal framework. Paleoceanography 8(6):737–766

Stocker TF, Johnsen SJ (2003) A minimum model for the bipolar seesaw. Paleoceanography 18 (4): 1087. DOI 10.1029/2003PA000920

Waelbroeck C, Labeyrie L, Michel E, Duplessy J-C, Mc Manus JF, Lambeck K, Balbon E, Labracherie M (2002) Sea level and deep temperature changes derived from benthic foraminifera benthic records. Quaternary Sci Rev 21:295–306

Wang Z, Mysak LA (2002) Simulation of the last glacial inception and rapid ice sheet growth in the McGill Paleoclimate Model. Geophys Res Let 29: DOI: 10.1029/2002GL015120